Letter

Exchange-phase erasure in anyonic Hong-Ou-Mandel interferometry

Sushanth Varada [1,2] Christian Spånslätt [3,1] and Matteo Acciai [4,1]

[1]*Department of Microtechnology and Nanoscience (MC2), Chalmers University of Technology, S-412 96 Göteborg, Sweden*

[2]*Department of Physics and Astronomy, Uppsala University, Box 516, S-751 20 Uppsala, Sweden*

[3]*Department of Engineering and Physics, Karlstad University, Karlstad, Sweden*

[4]*Scuola Internazionale Superiore di Studi Avanzati (SISSA), Via Bonomea 365, 34136 Trieste, Italy*

(Received 5 March 2025; revised 7 May 2025; accepted 14 May 2025; published 28 May 2025)

Two-particle interferometry is an important tool for extracting the exchange statistics of quantum particles. We theoretically investigate the prospects of such interferometry to probe the statistics of pointlike anyonic excitations injected in a Hong-Ou-Mandel (HOM) setup based on a quantum point contact device in the fractional quantum Hall regime. We compute the standard HOM ratio, i.e., the ratio of tunneling noises for two- and one-particle injections, and find that for pointlike anyons it only depends on the temperature and the anyon scaling dimension. Importantly, the latter is not necessarily related to the exchange phase. In fact, we establish that the HOM ratio does not reveal the exchange phase of the injected anyons: For injection-time delays that are small compared to the thermal timescale, we find that the exchange phase accumulated due to time-domain braiding between injected and thermally activated anyons is erased due to two mutually canceling subprocesses. In contrast, for time delays large compared to the thermal time, only a single subprocess contributes to the braiding, but the accumulated phase is canceled in the HOM ratio. These findings suggest caution when interpreting HOM interferometry experiments with anyons, and approaches beyond the standard HOM ratio are thus necessary to extract anyonic statistics with two-particle interferometry experiments.

DOI: 10.1103/PhysRevB.111.L201407

Introduction. Quantum exchange statistics is a tenet of modern physics, underpinning phenomena from Bose-Einstein condensation to the periodic table of elements to the formation of stars. In ordinary, three-dimensional space, quantum mechanics predicts [1] that elementary particles belong to one of two fundamental types: bosons and fermions. These types correspond to the many-body wave function of indistinguishable particles acquiring upon particle exchange a phase factor $e^{i\vartheta}$, with $\vartheta = 0$ and $\vartheta = \pi$ for bosons and fermions, respectively. Two-dimensional systems, however, permit particles beyond this dichotomy [2,3]. There, particle exchange can generate *any* phase angle ϑ and the particles are then referred to as (Abelian) anyons [4].

In this work, we investigate the prospects of detecting anyons with two-particle interferometry in the fractional quantum Hall (FQH) effect [5,6]. While the charges of FQH quasiparticles were established decades ago [7,8] to be fractions of the electron charge, it was only in 2020 that the FQH quasiparticles were experimentally established to be anyons [9,10]: In Ref. [10] an anyonic phase angle $\vartheta = \pi/3$ was observed in the FQH state at filling $\nu = 1/3$ in a Fabry-Pérot interferometer in the form of abrupt and reproducible phase jumps in the measured Aharonov-Bohm conductance patterns. This approach was later extended to other fillings in Refs. [11,12], and has recently been implemented also in graphene-based devices [13,14]. A complementary approach was taken in Ref. [9], which reported the impact of ϑ on the noise signal of a two-particle interferometer, in the so-called collider geometry. In that work, based on an earlier theoretical proposal [15], ϑ was proposed to affect the current correlations generated when two dilute beams of anyons carried by chiral edge states impinge on a beam splitter realized with a quantum point contact (QPC). This observation was later confirmed in additional, independent experiments [16–18], and has subsequently spurred several theoretical works [19–26]. The dominating interpretation of the collider experiments relies on the so-called "time-domain braiding" picture [27,28], where an exchange process involving impinging anyons and those spontaneously excited at the QPC provides a dominant, braiding contribution to the noise.

The anyon collider setup is similar to two-particle interferometry of Hong-Ou-Mandel (HOM) type, but with one important difference: In the anyon collider setup, the injected beams of particles are the result of random Poisson processes. In contrast, a HOM interferometer typically uses two controlled, time-delayed injections of particles onto the beam splitter. This setup was originally implemented for photons (bosons) [29], and was later extended to electrons (fermions) using QH edge states [30–39], for which interedge mode interactions [40–44] and channel mixing [45–48] can play a relevant role. A time-controlled anyonic HOM interferometer was only very recently reported [49], relying on simulating the injected anyonic states with voltage pulses, as proposed in Ref. [23].

In HOM interferometry, the quantum statistics of bosons and fermions is manifest as a peak and a dip, respectively, in

Published by the American Physical Society under the terms of the Creative Commons Attribution 4.0 International license. Further distribution of this work must maintain attribution to the author(s) and the published article's title, journal citation, and DOI. Funded by Bibsam.

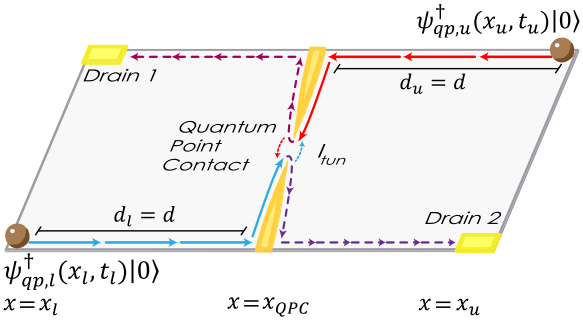


FIG. 1. Hong-Ou-Mandel interferometer realized in a fractional quantum Hall device setup. Pointlike anyonic states depicted by brown balls are injected at positions x_u, x_l in the upper (u) and lower (l) edges at times t_u and t_l, respectively. Drain terminals are used to detect the excess electronic noise S due to anyon interference at the collider quantum point contact at $x = x_{QPC}$. The distances d_u and d_l are for convenience both taken as d.

the so-called HOM ratio [see Eq. (14) below]. This quantity is given by the excess tunneling noise produced by two-particle injection, divided by the excess noise from single-particle injections, and quantifies the correlations of emitted particles in the two output channels of the interferometer. For bosons, the noise correlations are peaked around vanishing delay, as the Bose statistics produces a vanishing amplitude for output in two different channels when the particles simultaneously arrive at the beam splitter. By contrast, fermions produce a dip around vanishing delay, since the Pauli principle prevents two fermions from exiting in the same output state [33,50]. As (Abelian) anyons are in some sense intermediate between fermions and bosons, it is an interesting, open question how anyonic statistics might manifest in a HOM interferometer setup: a natural expectation is that HOM interferometry of anyons produces features intermediate between those observed for bosons and fermions, like a reduced dip in the HOM ratio. Indeed, a heuristic estimate of the probability of two anyons exiting a two-particle interferometer in different channels, due to different possible windings of the anyons around each other, can be associated with a statistical factor $(1 - \cos\vartheta)/2$ [51], which is intermediate between the bosonic ($\vartheta = 0$) and fermionic ($\vartheta = \pi$) scenarios. This factor, however, is based on braiding of anyons in real space, which does not occur in the simple pointlike QPC geometry usually considered in anyon colliders.

Here, we establish in detail that the expectation that the anyonic HOM ratio, realized with FQH edge modes in a standard QPC geometry, has "intermediate" features between bosons and fermions, is in fact incorrect. To this end, we consider the setup in Fig. 1, describing the injection of time-delayed, pointlike (i.e., with negligible time width) anyonic excitations in a QPC device in the FQH regime at filling $\nu = 1/m$ (with m an odd, positive integer). Such states have been shown to be experimentally relevant, as they can be simulated with ultrashort voltage pulses [23,49]. Our main finding is that for pointlike anyons the HOM ratio *does not* contain any information about the exchange phase of the injected anyons due to two effects: For small time delay, the total accumulated exchange phase, acquired from time-domain braiding between injected and thermally excited anyons at the QPC, is erased due to two competing subprocesses. For large time delay, the injected anyons braid instead independently with the thermally activated anyons, but this contribution cancels in the HOM ratio.

Setup and model. We consider the unperturbed, bosonized Hamiltonian [52] (we set $\hbar = 1$)

$$H_0 = \frac{v_F}{4\pi\nu}\int dx[[\partial_x\phi_{\rm u}(x)]^2 + [\partial_x\phi_{\rm l}(x)]^2], \tag{1}$$

where $\phi_{\rm u}$ and $\phi_{\rm l}$ are bosonic modes propagating to the left and to the right on the upper (u) and lower (l) edges (see Fig. 1), respectively. Both modes propagate with the velocity v_F and obey the commutation relations

$$[\phi_j(x), \phi_k(y)] = \mp i\pi\nu\delta_{jk}\,\mathrm{sgn}(x-y), \quad j,k = \mathrm{u},\mathrm{l}, \tag{2}$$

where δ_{jk} is the Kroenecker delta and $\mathrm{sgn}(x)$ is the sign function. Fractionalized quasiparticle excitations on the edges $j = \mathrm{u},\mathrm{l}$ are described by the vertex operators

$$\psi_{\mathrm{qp},j}(x) = \frac{F_j}{\sqrt{2\pi\alpha}}e^{-i\phi_j(x)}, \tag{3}$$

where α is a short-distance cutoff and F_j are the so-called Klein-factors, obeying the algebra $F_jF_j^\dagger = F_j^\dagger F_j = 1$ and $F_iF_j^\dagger = -F_j^\dagger F_i$ for $i \neq j$. In this work, however, Klein factors always appear in such a way that their product evaluates to unity and we thus ignore them in the following.

The charge densities propagating on the edges are given by

$$\rho_j(x) \equiv \mp q\frac{\partial_x\phi_j(x)}{2\pi}, \tag{4}$$

with $-$ for $j = \mathrm{l}$ and $+$ for $j = \mathrm{u}$ and where q is the electron charge. Equations (2)–(4) imply the following commutation relation between charge density and vertex operators:

$$[\rho_j(x), \psi^\dagger_{\mathrm{qp},j}(y)] = q\nu\delta(x-y)\psi^\dagger_{\mathrm{qp},j}(y). \tag{5}$$

Furthermore, combining Eqs. (2) and (3), one finds that exchanging the vertex operators $\psi_{\mathrm{qp},j}$ at different spatial coordinates results in an exchange phase factor according to

$$\psi_{\mathrm{qp},j}(x)\psi_{\mathrm{qp},j}(y) = \psi_{\mathrm{qp},j}(y)\psi_{\mathrm{qp},j}(x)e^{\pm i\vartheta\,\mathrm{sgn}(x-y)}, \tag{6}$$

with $+(-)$ for $j = \mathrm{u}\,(\mathrm{l})$. Moreover, vertex operators (3) with different j anticommute. We thus see that the operators (3) describe anyonic excitations with fractional charge $q\nu$ and, upon the identification $\vartheta = \pi\nu$, fractional statistics. These features stand in contrast to the electron excitations, i.e., excitations with charge q, which can be written in an analogous way to the fractional excitations of Eq. (3), namely

$$\psi_{\mathrm{el},j}(x) = \frac{F_j}{\sqrt{2\pi\alpha}}e^{-i\phi_j(x)/\nu}. \tag{7}$$

These operators can be checked to have the appropriate fermionic exchange phase $\vartheta = \pi$.

Next, to describe tunneling of quasiparticles at the quantum point contact (QPC) at $x = x_{\rm QPC}$, see Fig. 1, we add to H_0 the tunneling Hamiltonian

$$H_{\rm tun} = \Lambda A + \Lambda^* A^\dagger,$$
$$A = \psi^\dagger_{\mathrm{qp,u}}(x_{\rm QPC})\psi_{\mathrm{qp,l}}(x_{\rm QPC}). \tag{8}$$

Here, $|\Lambda| \ll 1$ is the weak tunneling amplitude, assumed to be energy independent, and A is a tunneling operator transferring quasiparticles between the two edges. Importantly, A can be interpreted as creating a quasiparticle-quasihole pair at the QPC. At finite temperature, these pairs are associated with thermal fluctuations; at zero temperature, they are associated with quantum fluctuations. A fundamental ingredient of the two-particle interferometer setup is a tunable injection of single anyonic excitations. In this work, we consider pointlike anyon injections, defined in terms of the state

$$|\varphi\rangle \equiv \psi^\dagger_{\mathrm{qp,u}}(x_\mathrm{u}, t_\mathrm{u})\psi^\dagger_{\mathrm{qp,l}}(x_\mathrm{l}, t_\mathrm{l})\,|0\rangle\,, \tag{9}$$

with $\psi^\dagger_{\mathrm{qp},j}(x)$ given in Eq. (3) and where $|0\rangle \equiv |0\rangle_\mathrm{u} \otimes |0\rangle_\mathrm{l}$ is the joint unperturbed, equilibrium ground state of the edges. The state (9) describes the injection of two point-like anyons (3) at the upper and lower edge locations x_u and x_l, at times t_u and t_l, respectively.

It was recently pointed out in Ref. [23] that the expressions for the tunneling currents and noise produced in the QPC by pointlike anyon injections are fully equivalent to the combined application of two specially tailored voltage pulses $V_j(t) = \frac{2\pi}{q}\delta(t - t_j)$. As long as the edge states have a linear dispersion, the injected voltage profiles do not disperse. In this way, the pointlike injection considered in this work can be experimentally *simulated* with voltage pulse injections, as previously studied in the context of QH edge states [34,53–58].

HOM noise and ratio. To analyze noise correlations and exchange statistics of anyons in the HOM setup, we next use the Hamiltonian $H_0 + H_\mathrm{tun}$ and perturbatively compute the tunneling current and noise.

To leading order in $|\Lambda|$, the tunneling current operator is given as [59]

$$I_\mathrm{tun} = iq\nu[\Lambda A(t) - \Lambda^* A^\dagger(t)], \tag{10}$$

where $A(t)$ is the time evolution in the interaction picture. In this work, operator expectation values are evaluated with respect to the auxiliary state (9), and will be denoted by $\langle\bullet\rangle_\varphi$. As will be clear below, however, such expectation values can be related to those with respect to the equilibrium state, $\langle\bullet\rangle_0$. We have

$$\begin{aligned}\langle A(t)A^\dagger(t')\rangle_0 &= \langle A^\dagger(t)A(t')\rangle_0 \\ &= \frac{1}{(2\pi\alpha)^2}\left[\frac{\pi k_B T\alpha/v_F}{i\sinh(\pi k_B T(t-t'-i\alpha/v_F))}\right]^{4\delta} \\ &= \frac{1}{(2\pi\alpha)^2}\left[\frac{\pi k_B T\alpha/v_F}{\sinh(\pi k_B T|t-t'|)}\right]^{4\delta} e^{-i2\pi\delta\,\mathrm{sgn}(t-t')}.\end{aligned} \tag{11}$$

Here, T is the temperature, k_B is the Boltzmann constant, and in the second line we used that the short distance cutoff $\alpha \ll 1$. The exponent δ is the so-called scaling dimension of the quasiparticle vertex operators (3), defined from the expression

$$\langle\psi^\dagger_{\mathrm{qp},j}(0,t)\psi_{\mathrm{qp},j}(0,0)\rangle_0 \sim t^{-2\delta}. \tag{12}$$

The scaling dimension thus governs the slow, characteristically power-law decay of the temporal correlations between quasiparticle-quasihole pairs at the QPC. Generically, δ is a nonuniversal parameter susceptible to a broad range of edge effects, e.g., interactions, disorder, neutral modes, and $1/f$ noise [60–67]. It is only in the ideal case with no such effects that δ is directly related to the FQH filling factor as $\nu = 2\delta$, as would be found from evaluating correlations functions of the operators (3) with respect to H_0. Since for ideal Laughlin states one universally has that $\vartheta = \pi\nu$, the absence of nonuniversal effects further implies that also the scaling dimension and the statistical exchange phase are directly related as $\vartheta = 2\pi\delta$. However, this relation cannot be expected to hold true in realistic devices, and discerning the nonuniversal effects of $2\pi\delta$ from ϑ is an essential experimental issue in detecting anyonic statistics. Throughout this work, we will therefore carefully distinguish the parameters δ and ϑ, and treat them as two independent variables.

The key quantity of interest in this work is the low-frequency noise [50,68] due to tunneling at the QPC in the FQH device. This noise is obtained from the correlation function of tunneling current operators (10) according to [59,69]

$$\begin{aligned}S &= \int_{-\infty}^{+\infty} dt \int_{-\infty}^{\infty} dt' \langle\{I_\mathrm{tun}(t), I_\mathrm{tun}(t')\}\rangle_\varphi \\ &= (q\nu|\Lambda|)^2 \int_{-\infty}^{+\infty} dt \int_{-\infty}^{\infty} dt' \langle\{A(t), A^\dagger(t')\} + \mathrm{H.c.}\rangle_\varphi\end{aligned} \tag{13}$$

where $\{X, Y\} = XY + YX$ is the anticommutator.

In the following, we are interested in the impact that simultaneous or close-to-simultaneous injections of quasiparticle excitations onto the QPC have on the noise. This effect is encoded in the so-called HOM noise, S_HOM, which is measured when anyons are injected on both edges. To isolate the tunneling noise from the background (thermal) noise, it is customary to subtract from S_HOM the background fluctuations S_eq, which are found from Eq. (13) by taking $\langle\bullet\rangle_\varphi \to \langle\bullet\rangle_0$. This subtraction defines the experimentally relevant *excess* HOM noise $\Delta S_\mathrm{HOM} = S_\mathrm{HOM} - S_\mathrm{eq}$. Furthermore, to quantify the effect of two injections, the excess HOM noise is normalized with the corresponding excess Hanbury Brown–Twiss (HBT) noise, $\Delta S_{\mathrm{HBT},j} \equiv S_{\mathrm{HBT},j} - S_\mathrm{eq}$, for $j = \mathrm{u}, \mathrm{l}$, which is obtained when anyons are injected on only one edge. The above procedures are jointly captured with the HOM-noise ratio [34,37,40]

$$\mathcal{R}(\tau_d) \equiv \frac{\Delta S_\mathrm{HOM}}{\Delta S_\mathrm{HBT,u} + \Delta S_\mathrm{HBT,l}}, \tag{14}$$

which is a function of the time delay $\tau_d \equiv t_\mathrm{l} - t_\mathrm{u}$ between the two anyon injections. The HOM-noise ratio (14) is the key quantity of interest in this work.

HOM interferometry with pointlike anyons. We now compute the tunneling noise (13) and then evaluate the HOM ratio (14). For the auxiliary state injection (9), the expressions for the tunneling noise involve nonequilibrium correlation functions of the form $\langle\varphi|A(t)A^\dagger(t')|\varphi\rangle$. To compute these functions, we use the fact that the state injection (9) is fully equivalent to shifting the vertex operators (3) with an additional creation of solitons in the bosonic modes ϕ_j. In other words, we perform the shifts [15,24]

$$\phi_{u/l}(x, t_{u/l}) \to \phi_{u/l}(x, t_{u/l}) + 2\vartheta\,\Theta[\mp x - v_F(t - t_{u/l}) \pm x_{u/l}], \tag{15}$$

with $\Theta(\bullet)$ the Heaviside function. The very same phase shifts arise from the voltage pulses discussed above [23]. At $x = x_{\rm QPC}$, the symmetric setup in Fig. 1 produces a constant offset $|x_{\rm QPC} - x_{\rm u,l}| = d_{\rm u,l} \equiv d$, which we absorb into the injection times $t_{\rm u,l}$. We then express the chiral evolution of the bosonic modes as

$$\phi_{\rm u,l}(t_{\rm u,l}) \to \phi_{\rm u,l}(t_{\rm u,l}) + 2\vartheta\,\Theta(t_{\rm u,l} - t). \tag{16}$$

By construction, the anyons injected into the upper and lower edges thus reach the QPC at the times $t = t_{\rm u,l}$, respectively. The shift (16) produces a phase factor in the non-equilibrium correlation function (11) and we find

$$\langle A(t)A^\dagger(t')\rangle_\varphi = \langle A(t)A^\dagger(t')\rangle_0 e^{i2\vartheta\,\Phi(t,t')}, \tag{17}$$

with the time-dependent phase component

$$\Phi(t,t') \equiv \Theta(t_{\rm u} - t) - \Theta(t_{\rm l} - t) + \Theta(t_{\rm l} - t') - \Theta(t_{\rm u} - t'). \tag{18}$$

We thus see that the phase factor in Eq. (17) manifests a fractional exchange phase $2\vartheta = 2\pi\nu$ which can be interpreted as braiding (i.e., a double exchange) between injected anyons and quasiparticle-quasihole pairs generated at the QPC.

By inserting the correlation function (17) into the tunneling noise (13), we obtain the excess HOM noise [70]

$$\Delta S_{\rm HOM} = \frac{4(2q\nu|\Lambda|)^2}{(2\pi\alpha)^2}(2\pi k_B T)^{4\delta-1}\left(\frac{\alpha}{v_F}\right)^{4\delta}\cos(2\pi\delta) \times [\cos(2\vartheta) - 1]\int_0^{|\tau_d|} dt\,\mathcal{B}(e^{-2\pi t/\beta}; 2\delta, \gamma). \tag{19}$$

In Eq. (19), $\mathcal{B}(x; a, b)$ is the incomplete Beta function, $\beta^{-1} \equiv k_B T$, $\gamma = 1 - 4\delta$, and $\tau_d \equiv t_{\rm l} - t_{\rm u}$ is the time delay. We see from Eq. (19) that the excess noise vanishes for zero time delay $\tau_d = 0$. This feature follows from Eq. (17) since (neglecting the energy dependence in the tunneling amplitude Λ and screening effects [71–74]), the device is in equilibrium at zero delay: $\langle A(t)A^\dagger(t')\rangle_\varphi = \langle A(t)A^\dagger(t')\rangle_0$. Moving on to the HOM ratio (14), we find that it can be written in compact form as [70]

$$\mathcal{R}(\tau_d) = 1 - \frac{\int_0^\infty dt\,\mathcal{B}(e^{-2\pi(t+|\tau_d|)/\beta}; 2\delta, \gamma)}{\int_0^\infty dt\,\mathcal{B}(e^{-2\pi t/\beta}; 2\delta, \gamma)}. \tag{20}$$

Crucially, we see that the anyon exchange phase ϑ is fully absent in the HOM ratio when point-like anyons are injected. Instead, the HOM ratio strongly depends on the scaling dimension δ of the quasiparticle-quasihole pairs excited at the QPC. This feature is shown in Fig. 2, where we plot $\mathcal{R}(\tau_d)$ for different values of δ. Besides the strong dependence on δ, the anyonic HOM ratio has another distinct feature not shared with noninteracting electrons, namely its temperature dependence. It was shown in Ref. [23] that the width of the HOM curves increases with decreasing temperature, in contrast to the free-electron case, where the width is set only by the temporal extension of the injected states, without any temperature dependence [32,38,70]. At small time delays $\tau_d \ll \beta$, Eq. (20) simplifies to [23]

$$\mathcal{R}(\tau_d) \approx 1 - e^{-|\tau_d|/\tau_{\rm th}}, \tag{21}$$

where the parameter $\tau_{\rm th} \equiv \beta/(4\pi\delta)$ defines a characteristic thermal timescale for anyon correlations, governing the QPC

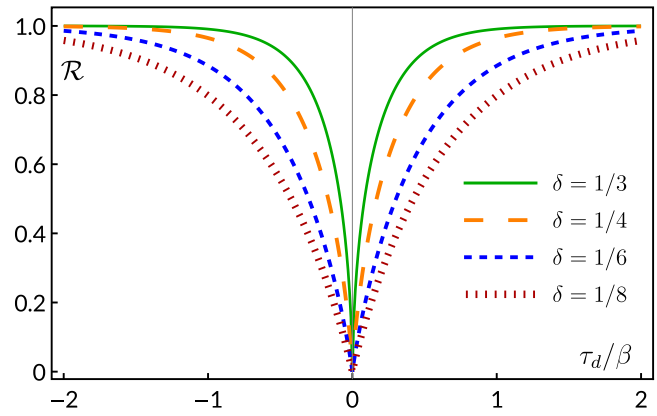


FIG. 2. Dimensionless HOM ratio $\mathcal{R}$ [Eq. (14)] as a function of the injection time delay $\tau_d \equiv t_{\rm l} - t_{\rm u}$ (in units of inverse temperature β), for several scaling dimensions δ.

quasiparticle-quasihole pair time correlations. Importantly, we see that this timescale does not involve ϑ but only δ. It follows that unlike for electrons and bosons, the standard HOM ratio (14) does not probe the exchange statistics angle ϑ of pointlike, injected anyons. We now elucidate why this is the case.

Exchange-phase erasure. The absence of the exchange phase ϑ in the standard HOM ratio (20) can be understood within the anyon time-domain braiding picture [28]. To illustrate this, we first rearrange the correlation function (17) as

$$\langle A(t)A^\dagger(t')\rangle_\varphi = \langle A(t)A^\dagger(t')\rangle_0 e^{i2\vartheta[\Theta(t_{\rm u}-t)-\Theta(t_{\rm u}-t')]}\, e^{i2\vartheta[\Theta(t_{\rm l}-t')-\Theta(t_{\rm l}-t)]}. \tag{22}$$

We also rewrite the tunneling noise (13) as

$$S \propto \int_{-\infty}^{\infty} dt\left(\int_t^\infty + \int_{-\infty}^t\right)dt' \sum_{k=\pm} {}_k\langle t, \tau_d|t', \tau_d\rangle_k + \text{H.c.} \tag{23}$$

Here, $|\bullet, \tau_d\rangle_- \equiv A(\bullet)\,|\varphi\rangle$ denotes the state with a quasiparticle created on the upper edge and a quasihole on the lower edge. Likewise, $|\bullet, \tau_d\rangle_+ \equiv A^\dagger(\bullet)\,|\varphi\rangle$ has a quasihole on the upper edge and a quasiparticle on the lower edge. We now begin by examining the contribution to the integral (23) for $t' > t$. In this range, the states $|t, \tau_d\rangle_-$ and $|t', \tau_d\rangle_-$ describe quasiparticle-quasihole excitations created *before* [Fig. 3(a)] and *after* [Fig. 3(b)] the arrival of the injected anyons at the QPC, respectively. Furthermore, the conjugated states ${}_-\langle t, \tau_d|$ and ${}_-\langle t', \tau_d|$ can be visually represented by rewinding the quasiparticle paths as shown in Figs. 4(a) and 4(b). In this way, the inner products of these states can be interpreted as time-domain interference loops where the injected anyons can braid with the QPC quasiparticle-quasihole excitations depending on the time delay τ_d.

Crucially, the time-domain braiding processes discussed above occur when at least one of the injection times $t_{\rm u}, t_{\rm l}$ falls within the window (t, t'). Of all possible intervals (t, t'), the most relevant ones are those for which $t' - t \lesssim \beta$, the contributions from others being suppressed by the decay of the correlation function. There are therefore three

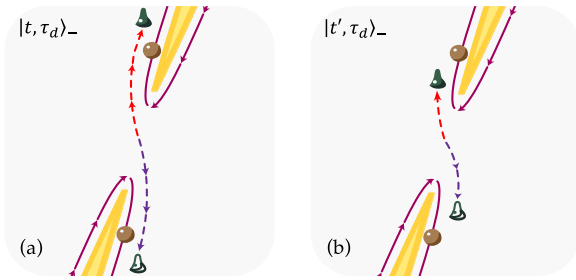


FIG. 3. Depiction of a tunneling subprocess that contributes to the noise in Eq. (23), here with $k = -$ and for $t' > t_u, t_l > t$. Injected anyons are depicted as brown balls with solid purple trajectories. Anyonic quasiparticle and quasiholes excited at the QPC are depicted by green peaks with dashed red trajectories and white peaks with dashed violet trajectories, respectively. (a) A quasiparticle-quasihole pair is excited at the QPC *before* the arrival of two injected anyons. (b) A quasiparticle-quasihole pair is excited *after* after the arrival of the injected anyons.

scenarios, as shown in Fig. 4(c): If the injection-time separation $\tau_d \ll \beta$, both t_u and t_l can fall in the window (t, t') and both injected anyons braid with the locally excited ones. However, the two anyons accumulate opposite braiding phases, resulting in a cancellation. If instead $\tau_d \gg \beta$, only one of the injected anyons can fall within the "braiding window,"

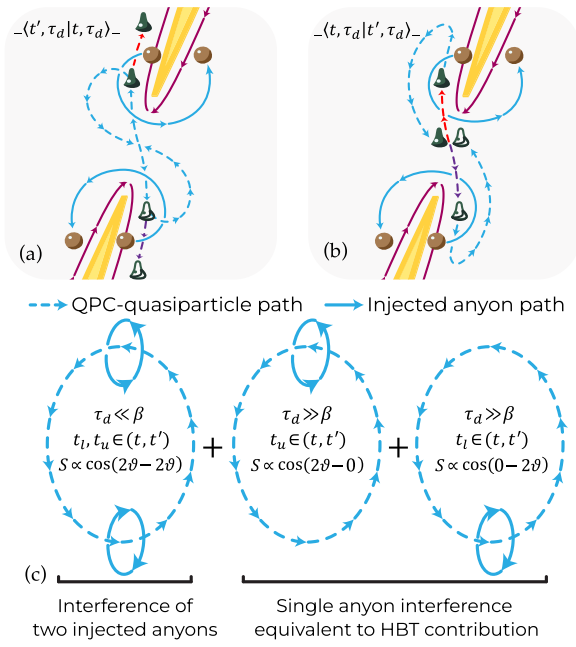


FIG. 4. Time-domain braiding amplitudes for the processes depicted in Fig. 3. (a) The amplitude is composed of Fig. 3(a) with the time reverse of Fig. 3(b). (b) The amplitude is composed of Fig. 3(b) with the time reverse of Fig. 3(a). The blue solid and dashed lines thus depict *time-reversed* paths of injected anyons and QPC quasiparticle-quasihole excitation, respectively. Trajectories at later times cross *above* trajectories at earlier times. (c) The braiding links to the left correspond to the two processes in (a) and (b). Exchange-phase effects in these processes for $\tau_d \ll \beta$ are erased from the HOM noise through counterbraiding in the time domain. The middle and right braiding links are formed when $\tau_d \gg \beta$ for single anyon injection, and are thus HBT contributions.

contributing to the noise with a term proportional to $\cos(2\vartheta)$. Only such processes contribute to the appearance of ϑ in S_{HOM} [75]. Moreover, at large time delays $\tau_d \gg \beta$, there are independent anyon injections on the two edges, which then corresponds to the HBT configuration. The same phase information is therefore contained in the numerator and denominator of the HOM ratio $\mathcal{R}(\tau_d)$, leading to the absence of ϑ in the HOM ratio, and resulting in Eq. (20). A perfectly analogous analysis holds for the second contribution in Eq. (23), namely, the time integral with $t' < t$. Figure 4(c) depicts the time-domain braiding subprocesses at the QPC for $k = -$. The analogous processes for $k = +$ are not drawn, but they are readily obtained by reversing the charge of the excited quasiparticles at the QPC.

According to the above analysis, we conclude that the counterbalancing braiding subprocesses, promoted by the anyonic long-time correlations, do not allow direct observation of the exchange statistics based on the standard HOM ratio. This is the main result of this work. We further remark that our derivation of the HOM ratio is not straightforward to adapt to noninteracting electrons by setting $\nu = 1$ and $\delta = 1/2$. As pointed out in Ref. [24], a bosonic shift (16) for $\nu = 1$ is equivalent to no shift at all. To obtain the HOM ratio in this case, one can use a bosonic shift with a small but nonvanishing temporal width [70]. In this way, the braiding becomes trivial $(2\vartheta = 2\pi)$ and one recovers that $\mathcal{R}$ gives the wavefunction overlap of the two injected single-electron states [32].

Summary and outlook. We studied two-particle interferometry of pointlike anyons in a fractional quantum Hall realization of the Hong-Ou-Mandel (HOM) interferometer setup. We found that, in contrast to bosons [29] and fermions [33], the characteristic HOM ratio $\mathcal{R}(\tau_d)$ [see Eq. (14)], with τ_d the injection-time delay, is void of the anyonic exchange phase ϑ. This result is essentially due to the peculiar nature of the FQH interferometer, that, to leading order in the tunneling amplitude, probes the time-domain braiding of the injected anyons with those excited at the QPC, rather then direct "collisions" of the incoming anyons [28]. More specifically, our detailed analysis showed that the origins of this absence lie in two complementary effects: When τ_d is small in comparison to the thermal timescale, the exchange phase accumulated from time-domain braiding between injected anyons and QPC quasiparticle-quasihole pairs is erased due to two subprocesses, whose phase contributions cancel exactly. Instead, for τ_d large compared to the thermal timescale, there are processes retaining the exchange phase, but their contributions are canceled in the HOM ratio $\mathcal{R}(\tau_d)$. This feature shows a clear difference between anyonic HOM interferometers and their fermionic/bosonic counterparts. Hence, extracting the anyonic phase from HOM interferometry requires going beyond the standard HOM ratio and implement more sophisticated measurement protocols. One such approach was recently investigated in Ref. [49], where estimates of both scaling dimension and the anyonic exchange phase were provided from combined measurements of the tunneling conductance and noise.

As a natural followup of our work, it would be interesting to investigate whether a full exchange-phase cancellation in the HOM ratio persists for finite-width anyon states [24–26]. Additionally, it remains an open question whether a wavefunction description of anyonic levitons [76] can be related

to the weak backscattering HOM noise considered in this work. Another natural direction is to investigate whether there are possibilities to extract the statistics of anyons on more complex edges, e.g., at fillings $\nu = 2/5$ or $\nu = 2/3$, whose description requires taking into account non-topological edge effects, e.g., interactions, disorder, and equilibration [77–81].

Note added. Some of the results in this paper have been reported in the Master's thesis in Ref. [82].

Acknowledgments. We gratefully acknowledge Janine Splettstoesser for discussions and feedback on the manuscript. This project has received funding from the European Union's Horizon 2020 research and innovation programme under Grant Agreements No. 862683 (FET-OPEN UltraFastNano) and No. 101031655 (TEAPOT). We also acknowledge funding from the Swedish Vetenskapsrådet via Project No. 2023-04043 (C.S.), from the Area of Advance Nano at Chalmers University of Technology (C.S.), and from the PNRR MUR Project No. PE0000023-NQSTI (M.A.).

Data availability. The data that support the findings of this article are openly available [83].

[1] M. G. G. Laidlaw and C. M. DeWitt, Feynman Functional integrals for systems of indistinguishable particles, Phys. Rev. D **3**, 1375 (1971).

[2] J. M. Leinaas and J. Myrheim, On the theory of identical particles, Nuovo Cimento B **37**, 1 (1977).

[3] G. A. Goldin, R. Menikoff, and D. H. Sharp, Particle statistics from induced representations of a local current group, J. Math. Phys. **21**, 650 (1980).

[4] F. Wilczek, Quantum mechanics of fractional-spin particles, Phys. Rev. Lett. **49**, 957 (1982).

[5] D. C. Tsui, H. L. Stormer, and A. C. Gossard, Two-dimensional magnetotransport in the extreme quantum limit, Phys. Rev. Lett. **48**, 1559 (1982).

[6] R. B. Laughlin, Anomalous quantum Hall effect: An incompressible quantum fluid with fractionally charged excitations, Phys. Rev. Lett. **50**, 1395 (1983).

[7] R. De-Picciotto, M. Reznikov, M. Heiblum, V. Umansky, G. Bunin, and D. Mahalu, Direct observation of a fractional charge, Nature (London) **389**, 162 (1997).

[8] L. Saminadayar, D. C. Glattli, Y. Jin, and B. Etienne, Observation of the $e/3$ fractionally charged Laughlin quasiparticle, Phys. Rev. Lett. **79**, 2526 (1997).

[9] H. Bartolomei, M. Kumar, R. Bisognin, A. Marguerite, J.-M. Berroir, E. Bocquillon, B. Plaçais, A. Cavanna, Q. Dong, U. Gennser, Y. Jin, and G. Fève, Fractional statistics in anyon collisions, Science **368**, 173 (2020).

[10] J. Nakamura, S. Liang, G. C. Gardner, and M. J. Manfra, Direct observation of anyonic braiding statistics, Nat. Phys. **16**, 931 (2020).

[11] J. Nakamura, S. Liang, G. C. Gardner, and M. J. Manfra, Impact of bulk-edge coupling on observation of anyonic braiding statistics in quantum Hall interferometers, Nat. Commun. **13**, 344 (2022).

[12] J. Nakamura, S. Liang, G. C. Gardner, and M. J. Manfra, Fabry-Pèrot interferometry at the $\nu = 2/5$ fractional quantum Hall state, Phys. Rev. X **13**, 041012 (2023).

[13] N. L. Samuelson, L. A. Cohen, W. Wang, S. Blanch, T. Taniguchi, K. Watanabe, M. P. Zaletel, and A. F. Young, Anyonic statistics and slow quasiparticle dynamics in a graphene fractional quantum Hall interferometer, arXiv:2403.19628.

[14] T. Werkmeister, J. R. Ehrets, M. E. Wesson, D. H. Najafabadi, K. Watanabe, T. Taniguchi, B. I. Halperin, A. Yacoby, and P. Kim, Anyon braiding and telegraph noise in a graphene interferometer, Science **388**, 730 (2025).

[15] B. Rosenow, I. P. Levkivskyi, and B. I. Halperin, Current correlations from a mesoscopic anyon collider, Phys. Rev. Lett. **116**, 156802 (2016).

[16] M. Ruelle, E. Frigerio, J.-M. Berroir, B. Plaçais, J. Rech, A. Cavanna, U. Gennser, Y. Jin, and G. Fève, Comparing fractional quantum Hall Laughlin and Jain topological orders with the anyon collider, Phys. Rev. X **13**, 011031 (2023).

[17] P. Glidic, O. Maillet, A. Aassime, C. Piquard, A. Cavanna, U. Gennser, Y. Jin, A. Anthore, and F. Pierre, Cross-correlation investigation of anyon statistics in the $\nu = 1/3$ and $2/5$ fractional quantum Hall states, Phys. Rev. X **13**, 011030 (2023).

[18] J.-Y. M. Lee, C. Hong, T. Alkalay, N. Schiller, V. Umansky, M. Heiblum, Y. Oreg, and H.-S. Sim, Partitioning of diluted anyons reveals their braiding statistics, Nature (London) **617**, 277 (2023).

[19] T. Morel, J.-Y. M. Lee, H.-S. Sim, and C. Mora, Fractionalization and anyonic statistics in the integer quantum Hall collider, Phys. Rev. B **105**, 075433 (2022).

[20] J.-Y. M. Lee, C. Han, and H.-S. Sim, Fractional mutual statistics on integer quantum Hall edges, Phys. Rev. Lett. **125**, 196802 (2020).

[21] J.-Y. M. Lee and H.-S. Sim, Non-Abelian anyon collider, Nat. Commun. **13**, 1 (2022).

[22] E. G. Idrisov, I. P. Levkivskyi, E. V. Sukhorukov, and T. L. Schmidt, Current cross correlations in a quantum Hall collider at filling factor two, Phys. Rev. B **106**, 085405 (2022).

[23] T. Jonckheere, J. Rech, B. Grémaud, and T. Martin, Anyonic statistics revealed by the Hong-Ou-Mandel dip for fractional excitations, Phys. Rev. Lett. **130**, 186203 (2023).

[24] N. Schiller, Y. Shapira, A. Stern, and Y. Oreg, Anyon statistics through conductance measurements of time-domain interferometry, Phys. Rev. Lett. **131**, 186601 (2023).

[25] K. Iyer, F. Ronetti, B. Grémaud, T. Martin, J. Rech, and T. Jonckheere, Finite width of anyons changes their braiding signature, Phys. Rev. Lett. **132**, 216601 (2024).

[26] M. Thamm and B. Rosenow, Effect of the soliton width on nonequilibrium exchange phases of anyons, Phys. Rev. Lett. **132**, 156501 (2024).

[27] C. Han, J. Park, Y. Gefen, and H.-S. Sim, Topological vacuum bubbles by anyon braiding, Nat. Commun. **7**, 11131 (2016).

[28] B. Lee, C. Han, and H.-S. Sim, Negative excess shot noise by anyon braiding, Phys. Rev. Lett. **123**, 016803 (2019).

[29] C. K. Hong, Z. Y. Ou, and L. Mandel, Measurement of subpicosecond time intervals between two photons by interference, Phys. Rev. Lett. **59**, 2044 (1987).

[30] S. Ol'khovskaya, J. Splettstoesser, M. Moskalets, and M. Büttiker, Shot noise of a mesoscopic two-particle collider, Phys. Rev. Lett. **101**, 166802 (2008).

[31] E. Bocquillon, F. D. Parmentier, C. Grenier, J.-M. Berroir, P. Degiovanni, D. C. Glattli, B. Plaçais, A. Cavanna, Y. Jin, and

G. Fève, Electron quantum optics: Partitioning electrons one by one, Phys. Rev. Lett. **108**, 196803 (2012).

[32] T. Jonckheere, J. Rech, C. Wahl, and T. Martin, Electron and hole Hong-Ou-Mandel interferometry, Phys. Rev. B **86**, 125425 (2012).

[33] E. Bocquillon, V. Freulon, J.-M. Berroir, P. Degiovanni, B. Plaçais, A. Cavanna, Y. Jin, and G. Fève, Coherence and Indistinguishability of single electrons emitted by independent sources, Science **339**, 1054 (2013).

[34] J. Dubois, T. Jullien, C. Grenier, P. Degiovanni, P. Roulleau, and D. C. Glattli, Integer and fractional charge Lorentzian voltage pulses analyzed in the framework of photon-assisted shot noise, Phys. Rev. B **88**, 085301 (2013).

[35] J. Dubois, T. Jullien, F. Portier, P. Roche, A. Cavanna, Y. Jin, W. Wegscheider, P. Roulleau, and D. C. Glattli, Minimal-excitation states for electron quantum optics using levitons, Nature (London) **502**, 659 (2013).

[36] D. Ferraro, A. Feller, A. Ghibaudo, E. Thibierge, E. Bocquillon, G. Fève, Ch. Grenier, and P. Degiovanni, Wigner function approach to single electron coherence in quantum Hall edge channels, Phys. Rev. B **88**, 205303 (2013).

[37] E. Bocquillon, V. Freulon, F. D. Parmentier, J.-M. Berroir, B. Plaçais, C. Wahl, J. Rech, T. Jonckheere, T. Martin, C. Grenier, D. Ferraro, P. Degiovanni, and G. Fève, Electron quantum optics in ballistic chiral conductors, Ann. Phys. **526**, 1 (2014).

[38] D. C. Glattli and P. Roulleau, Hanbury-Brown Twiss noise correlation with time controlled quasi-particles in ballistic quantum conductors, Physica E **76**, 216 (2016).

[39] A. Marguerite, E. Bocquillon, J.-M. Berroir, B. Plaçais, A. Cavanna, Y. Jin, P. Degiovanni, and G. Fève, Two-particle interferometry in quantum Hall edge channels, Phys. Status Solidi B **254**, 1600618 (2017).

[40] C. Wahl, J. Rech, T. Jonckheere, and T. Martin, Interactions and charge fractionalization in an electronic Hong-Ou-Mandel interferometer, Phys. Rev. Lett. **112**, 046802 (2014).

[41] V. Freulon, A. Marguerite, J.-M. Berroir, B. Plaçais, A. Cavanna, Y. Jin, and G. Fève, Hong-Ou-Mandel experiment for temporal investigation of single-electron fractionalization, Nat. Commun. **6**, 6854 (2015).

[42] A. Marguerite, C. Cabart, C. Wahl, B. Roussel, V. Freulon, D. Ferraro, Ch. Grenier, J.-M. Berroir, B. Plaçais, T. Jonckheere, J. Rech, T. Martin, P. Degiovanni, A. Cavanna, Y. Jin, and G. Fève, Decoherence and relaxation of a single electron in a one-dimensional conductor, Phys. Rev. B **94**, 115311 (2016).

[43] C. Cabart, B. Roussel, G. Fève, and P. Degiovanni, Taming electronic decoherence in one-dimensional chiral ballistic quantum conductors, Phys. Rev. B **98**, 155302 (2018).

[44] G. Rebora, M. Acciai, D. Ferraro, and M. Sassetti, Collisional interferometry of levitons in quantum Hall edge channels at $\nu = 2$, Phys. Rev. B **101**, 245310 (2020).

[45] I. Taktak, M. Kapfer, J. Nath, P. Roulleau, M. Acciai, J. Splettstoesser, I. Farrer, D. A. Ritchie, and D. C. Glattli, Two-particle time-domain interferometry in the fractional quantum Hall effect regime, Nat. Commun. **13**, 5863 (2022).

[46] M. Acciai, P. Roulleau, I. Taktak, D. C. Glattli, and J. Splettstoesser, Influence of channel mixing in fermionic Hong-Ou-Mandel experiments, Phys. Rev. B **105**, 125415 (2022).

[47] M. Acciai, P. Roulleau, D. C. Glattli, and J. Splettstoesser, Impact of channel mixing on the visibility of two-particle interferometry in quantum Hall edge states, JPS Conf. Proc. **38**, 011174 (2023).

[48] D. C. Glattli, A. De, C. Boudet, M. Kapfer, I. Farrer, D. Ritchie, and P. Roulleau, Electronic Hong Ou Mandel interferences to unveil the 2/3 fractional quantum Hall edge channel dynamics, Research Square preprint (2025).

[49] M. Ruelle, E. Frigerio, E. Baudin, J.-M. Berroir, B. Plaçais, B. Grémaud, T. Jonckheere, T. Martin, J. Rech, A. Cavanna, U. Gennser, Y. Jin, G. Ménard, and G. Fève, Time-domain braiding of anyons, arXiv:2409.08685.

[50] Ya. M. Blanter and M. Büttiker, Shot noise in mesoscopic conductors, Phys. Rep. **336**, 1 (2000).

[51] G. Campagnano, O. Zilberberg, I. V. Gornyi, D. E. Feldman, A. C. Potter, and Y. Gefen, Hanbury Brown–Twiss interference of anyons, Phys. Rev. Lett. **109**, 106802 (2012).

[52] X.-G. Wen, Topological orders and edge excitations in fractional quantum Hall states, Adv. Phys. **44**, 405 (1995).

[53] M. Moskalets, First-order correlation function of a stream of single-electron wave packets, Phys. Rev. B **91**, 195431 (2015).

[54] J. Rech, D. Ferraro, T. Jonckheere, L. Vannucci, M. Sassetti, and T. Martin, Minimal excitations in the fractional quantum Hall regime, Phys. Rev. Lett. **118**, 076801 (2017).

[55] L. Vannucci, F. Ronetti, J. Rech, D. Ferraro, T. Jonckheere, T. Martin, and M. Sassetti, Minimal excitation states for heat transport in driven quantum Hall systems, Phys. Rev. B **95**, 245415 (2017).

[56] F. Ronetti, L. Vannucci, D. Ferraro, T. Jonckheere, J. Rech, T. Martin, and M. Sassetti, Crystallization of levitons in the fractional quantum Hall regime, Phys. Rev. B **98**, 075401 (2018).

[57] D. Ferraro, F. Ronetti, L. Vannucci, M. Acciai, J. Rech, T. Jockheere, T. Martin, and M. Sassetti, Hong-Ou-Mandel characterization of multiply charged Levitons, Eur. Phys. J. Spec. Top. **227**, 1345 (2018).

[58] F. Ronetti, L. Vannucci, D. Ferraro, T. Jonckheere, J. Rech, T. Martin, and M. Sassetti, Hong-Ou-Mandel heat noise in the quantum Hall regime, Phys. Rev. B **99**, 205406 (2019).

[59] T. Martin, Noise in mesoscopic physics, in *Nanophysics: Coherence and Transport*, edited by H. Bouchiat, Y. Gefen, S. Guéron, G. Montambaux, and J. Dalibard, Les Houches Vol. 81 (Elsevier, Waltham, MA, 2005), pp. 283–359.

[60] C. L. Kane and M. P. A. Fisher, Transmission through barriers and resonant tunneling in an interacting one-dimensional electron gas, Phys. Rev. B **46**, 15233 (1992).

[61] L. P. Pryadko, E. Shimshoni, and A. Auerbach, Coulomb interactions and delocalization in quantum Hall constrictions, Phys. Rev. B **61**, 10929 (2000).

[62] B. Rosenow and B. I. Halperin, Nonuniversal behavior of scattering between fractional quantum Hall Edges, Phys. Rev. Lett. **88**, 096404 (2002).

[63] E. Papa and A. H. MacDonald, Interactions suppress quasiparticle tunneling at Hall bar constrictions, Phys. Rev. Lett. **93**, 126801 (2004).

[64] D. Ferraro, A. Braggio, M. Merlo, N. Magnoli, and M. Sassetti, Relevance of multiple quasiparticle tunneling between edge states at $\nu = p/(2np+1)$, Phys. Rev. Lett. **101**, 166805 (2008).

[65] A. Braggio, D. Ferraro, M. Carrega, N. Magnoli, and M. Sassetti, Environmental induced renormalization effects in quantum Hall edge states due to 1/f noise and dissipation, New J. Phys. **14**, 093032 (2012).

[66] R. Kumar, S. K. Srivastav, C. Spånslätt, K. Watanabe, T. Taniguchi, Y. Gefen, A. D. Mirlin, and A. Das, Observation of ballistic upstream modes at fractional quantum Hall edges of graphene, Nat. Commun. **13**, 213 (2022).

[67] M. Acciai, G. Zhang, and C. Spånslätt, Role of scaling dimensions in generalized noises in fractional quantum Hall tunneling due to a temperature bias, SciPost Phys. **18**, 058 (2025).

[68] K. Kobayashi and M. Hashisaka, Shot noise in mesoscopic systems: From single particles to quantum liquids, J. Phys. Soc. Jpn. **90**, 102001 (2021).

[69] For correct units of noise, one should in principle replace the integration over t in Eq. (13) by $\int_{-\mathcal{T}_0/2}^{\mathcal{T}_0/2} dt/\mathcal{T}_0$, with $\mathcal{T}_0$ a very long averaging time. This replacement, however, has no impact on the dimensionless HOM ratio (14).

[70] See Supplemental Material at http://link.aps.org/supplemental/10.1103/PhysRevB.111.L201407 which includes details on (i) the derivation of the HOM ratio and (ii) a comparison to HOM interferometry of electrons.

[71] T. Christen and M. Büttiker, Low frequency admittance of a quantum point contact, Phys. Rev. Lett. **77**, 143 (1996).

[72] A. Prêtre, H. Thomas, and M. Büttiker, Dynamic admittance of mesoscopic conductors: Discrete-potential model, Phys. Rev. B **54**, 8130 (1996).

[73] J. Meair and P. Jacquod, Scattering theory of nonlinear thermoelectricity in quantum coherent conductors, J. Phys.: Condens. Matter **25**, 082201 (2013).

[74] N. Dashti, M. Acciai, S. Kheradsoud, M. Misiorny, P. Samuelsson, and J. Splettstoesser, Readout of quantum screening effects using a time-dependent probe, Phys. Rev. Lett. **127**, 246802 (2021).

[75] However, ϑ appears in the noise jointly with the scaling dimension δ, making an extraction of only ϑ challenging.

[76] H.-S. Sim (private communication).

[77] C. L. Kane, M. P. A. Fisher, and J. Polchinski, Randomness at the edge: Theory of quantum Hall transport at filling $\nu = 2/3$, Phys. Rev. Lett. **72**, 4129 (1994).

[78] I. Protopopov, Y. Gefen, and A. Mirlin, Transport in a disordered $\nu = 2/3$ fractional quantum Hall junction, Ann. Phys. **385**, 287 (2017).

[79] C. Nosiglia, J. Park, B. Rosenow, and Y. Gefen, Incoherent transport on the $\nu = 2/3$ quantum Hall edge, Phys. Rev. B **98**, 115408 (2018).

[80] C. Spånslätt, Y. Gefen, I. V. Gornyi, and D. G. Polyakov, Contacts, equilibration, and interactions in fractional quantum Hall edge transport, Phys. Rev. B **104**, 115416 (2021).

[81] M. Hein and C. Spånslätt, Thermal conductance and noise of Majorana modes along interfaced $\nu = \frac{5}{2}$ fractional quantum Hall states, Phys. Rev. B **107**, 245301 (2023).

[82] S. Varada, Anyon colliders: A time-dependent quantum Hall particle collider to reveal fractional statistics in the Laughlin sequence, Master's thesis, Chalmers University of Technology, 2023.

[83] S. Varada, C. Spånslätt, and M. Acciai, Data for "Exchange-phase erasure in anyonic Hong-Ou-Mandel interferometry", Zenodo (2025), doi: 10.5281/zenodo.15356728.